NANO LETTERS

Letter

pubs.acs.org/NanoLett

Active Chiral Plasmonics

Xinghui Yin,*[†,§] Martin Schäferling,[†] Ann-Katrin U. Michel,[‡] Andreas Tittl,[†] Matthias Wuttig,[‡] Thomas Taubner,[‡] and Harald Giessen[†]

[†]4th Physics Institute and Research Center SCoPE, University of Stuttgart, 70550, Stuttgart, Germany

[‡]I. Institute of Physics (IA), RWTH Aachen University, 52056, Aachen, Germany

[§]Max Planck Institute for Solid State Research, Heisenbergstrasse 1, D-70569 Stuttgart, Germany

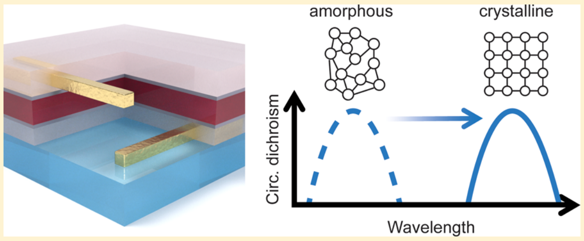

ABSTRACT: Active control over the handedness of a chiral metamaterial has the potential to serve as key element for highly integrated polarization engineering approaches, polarization sensitive imaging devices, and stereo display technologies. However, this is hard to achieve as it seemingly involves the reconfiguration of the metamolecule from a left-handed into a right-handed enantiomer and vice versa. This type of mechanical actuation is intricate and usually neither monolithically realizable nor viable for high-speed applications. Here, enabled by the phase change material $Ge_3Sb_2Te_6$ (GST-326), we demonstrate a tunable and switchable mid-infrared plasmonic chiral metamaterial in a proof-of-concept experiment. A large tunability range of the circular dichroism response from $\lambda = 4.15$ to 4.90 μm is achieved, and we experimentally demonstrate that the combination of a passive bias-type chiral layer with the active chiral metamaterial allows for switchable chirality, that is, the reversal of the circular dichroism sign, in a fully planar, layered design without the need for geometrical reconfiguration. Because phase change materials can be electrically and optically switched, our designs may open up a path for highly integrated mid-IR polarization engineering devices that can be modulated on ultrafast time scales.

KEYWORDS: *Switchable, tunable, chirality, plasmonic, phase change material, metamaterial*

The first metamaterials comprising of plasmonic structures were fully static, that is, their geometry, material, dielectric environment, and hence optical properties were fixed by design. However, introducing handles for postfabrication control over plasmonic optical mode behavior is crucial for pushing metamaterials into the domain of reconfigurable devices[1] for applications as varied as all-optical nanophotonic circuits, imaging, sensors, data storage and displays. The most obvious feature one can tune is the spectral position of the plasmon resonance frequency. To this end, mechanical means that effect a deformation of the artificial material,[2,3] graphene[4−7] injection of free carriers in semiconductors,[8−12] and materials such as VO_2,[13−15] gallium,[16,17] yttrium-hydride,[18] and the phase change material GeSbTe (GST)[19−21] have been successfully employed. A less accessible but very important characteristic that lends itself to external control is chirality. Optically, chirality manifests itself in a circular dichroism (CD) signal, that is, a difference in absorption of left-handed and right-handed circularly polarized light, which has opposite signs for mirror image pairs of metamolecules, so-called enantiomers. A large body of work exists on chiral metamaterials in the optical,[22−27] infrared,[27−33] terahertz (THz),[34−37] and gigahertz (GHz)[38] regimes. Yet, comparably few demonstrations exist for switchable chiral metamaterials that can change their handedness under the influence of an external stimulus. Generally, reconfiguring the chiral building block such that it geometrically switches between the enantiomers will lead to a symmetric change in the CD signal, which has been demonstrated in the visible spectral region using solution-based DNA-self-assembled chiral structures.[39] In the THz spectral regime, the generation of charge carriers through optical excitation in silicon was utilized to selectively activate certain parts of an overall achiral geometry to obtain an either positive or negative CD signal.[40−43] These approaches are not available in the mid-infrared (MIR), which, however, is a highly interesting spectral region for plasmonics,[44] for example, due to the presence of molecular vibrational fingerprints and the atmospheric transparency window.

Here, we first experimentally demonstrate large spectral tunability of the circular dichroism response, and subsequently utilize this effect in combination with a passive chiral bias-type layer to obtain switching of the CD signal sign in the MIR. To achieve this, we employ the chalcogenide phase change material $Ge_3Sb_2Te_6$ (GST-326), which is a representative of the chalcogenide compound family that has been successfully commercialized for optical data storage (DVDs) and recently received additional attention due to its exciting electro-optical properties that make it suitable as a new low energy, high contrast display material.[45]

Plasmon resonances in metal nanostructures are very sensitive to their immediate dielectric environment, which has been extensively used for sensing purposes.[46,47] When GST-

Received: November 4, 2014
Revised: January 6, 2015
Published: June 3, 2015

DOI: 10.1021/nl5042325
Nano Lett. 2015, 15, 4255−4260

326 is brought into proximity with a plasmonic nanoantenna, the large difference in the dielectric constant between amorphous ($\tilde{n}_a \approx 3.5 + 0.01i$) and crystalline ($\tilde{n}_c \approx 6.5 + 0.06i$) GST-326[20] in the studied mid infrared spectral region (4−5 μm) leads to a large spectral shift of the particle plasmon resonance position. Therefore, a suitable combination of GST with a chiral metamaterial leads to a shifted circular dichroism signal upon actuation[48] (Figure 1b). We choose a Born-Kuhn type chiral plasmonic dimer[33,49,50] as underlying system and modify it by sandwiching a thin layer of GST-326 between the two corner-stacked nanorods (Figure 1a). This has the two-fold advantage of ensuring an optimum interaction with the nanorods, because the phase change layer is incorporated at the near-field coupling junction and ease of fabrication, because no additional lithography step is needed. The fabrication steps follow a modified recipe of the stacking procedure from ref 51 and are outlined in Figure 2: a first electron beam lithography step is carried out to define alignment markers and the first layer of the chiral dimer (Figure 2a). The length of the nanorods is $l = 660$ nm, the width $w = 40$ nm, and the thickness = 50 nm. A C_4-symmetric supercell of chiral dimers is placed in a disordered arrangement over a 100 μm × 100 μm area in order to avoid Rayleigh anomalies in the high-index case. As substrate, we use CaF_2 to ensure mid-IR transparency. The spin-on polymer PC403 (JSR Inc., Japan) is applied as a 60 nm thick planarization layer and subsequently a 50 nm GST-326 layer sandwiched between 10 nm buffer layers of ZnS/SiO$_2$ is dc-magnetron sputter deposited. A second step of aligned electron beam lithography is carried out to define the upper nanorods, which are finally covered by 100 nm of PC403 to symmetrize the dielectric environment. The resulting SEM micrograph for a right-handed active structure is shown in Figure 2e. The lattice spacing is deliberately randomized in order to avoid Rayleigh anomalies in the optical spectra.[52,53]

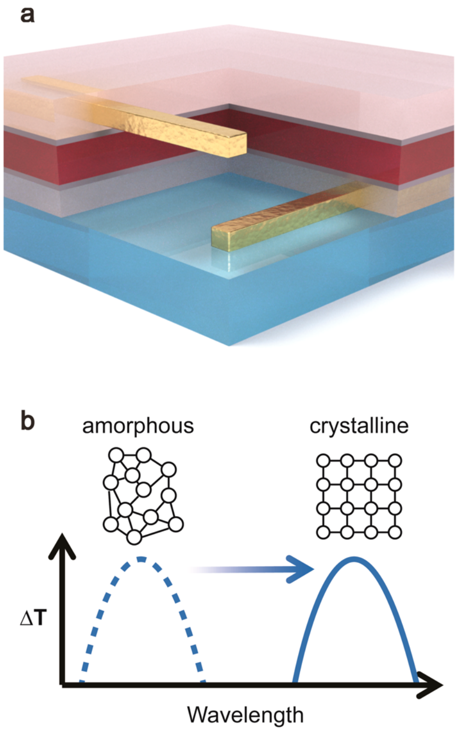

Figure 1. Tunable chirality concept. (a) Active chiral plasmonic dimer stack consisting of 50 nm GST-326 (red) with two protective10 nm ZnS/SiO$_2$ layers (gray) sandwiched between vertically displaced, corner-stacked, orthogonal gold nanorods embedded in PC403 (light red). For better visibility of the nanorods, a cut-away is included at the edge of the stack. (b) Thermal actuation of the phase change layer leads to a CD signal ΔT that is shifted to longer wavelengths.

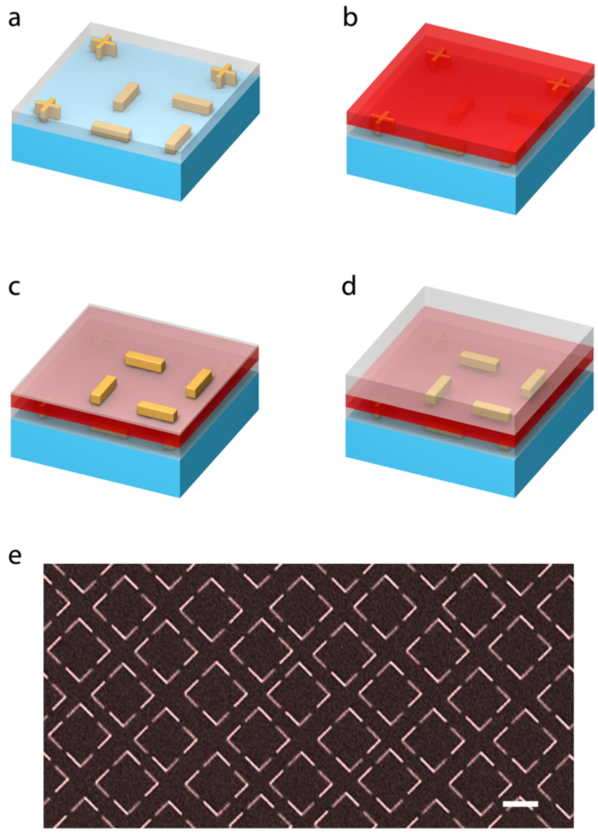

Figure 2. Fabrication flowchart. (a) First electron beam lithography (EBL) step creates markers and the first layer of Au nanorods (50 nm). Spin-coating of a planarization layer consisting of PC403 (gray, 60 nm) smooths the surface. (b) Sputter deposition of GST-326 (red) sandwiched between two thin protective layers of ZnS/SiO$_2$ (10 nm). (c) Spin-coating of PC403 layer (10 nm) followed by second aligned EBL step defining the upper nanorods. (d) Spin-coating of PC403 planarization layer (140 nm) to symmetrize the dielectric environment. (e) SEM micrograph of fabricated right-handed structure (scale bar = 1 μm). The top layer appears brighter. The irregular lattice spacing is used to avoid Rayleigh anomalies.

The structure parameters of the fabricated sample were chosen such that the fundamental plasmon resonance is located in the transparency window[20] of GST-326, that is, between 2.8 and 5.5 μm for both the amorphous and the crystalline phase where absorption losses of such a thin film are negligibly small (≪1%). To guide the design and predict the tuning behavior of the active chiral dimer, we carried out electromagnetic full-field simulations for the system described above including all layers with periodic supercells of period $p = 1600$ nm employing an in house-implementation of the Fourier modal method.[54]

The results are shown in Figure 3a, where lighter-colored curves represent spectra for the GST-326 layer in the amorphous phase and darker-colored curves are associated with the crystalline phase. For both states, the transmittance spectra for a right-handed enantiomer under illumination with circularly polarized light are shown in the upper plot. One can clearly see that left- and right- circularly polarized light is transmitted differently, thus confirming the chiroptical nature of

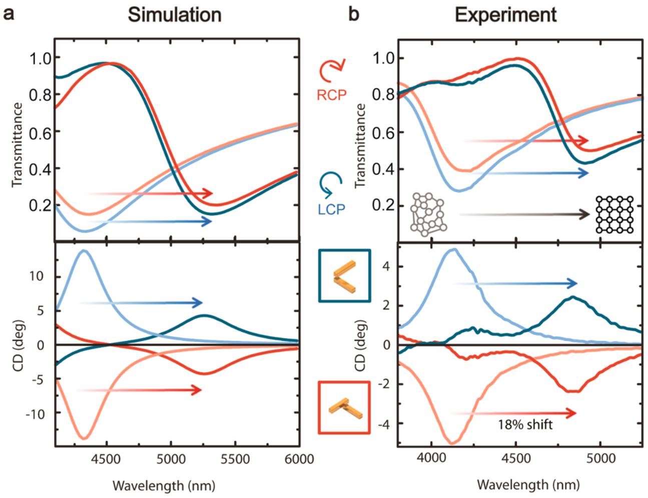

Figure 3. Tunable chirality experiment and simulation. (a) Simulated transmittance (upper panel) and CD (lower panel) spectra through the active chiral dimer of left- and right-handed circularly polarized light for the amorphous (lighter curves) and crystalline (darker curves) state of the phase change material layer. (b) Corresponding spectra to (a) from FTIR measurements of the fabricated sample.

the investigated system. Additionally, a giant spectral shift of around 20% is obtained in the simulation when the sandwich layer undergoes a phase change from the amorphous to the crystalline state. The lower plot shows the CD spectra for both right- and left-handed enantiomers in degrees, where the formula $\theta(\text{deg}) = 33(\log(T_{\text{RCP}}) - \log(T_{\text{LCP}}))$ was used for the conversion from the transmittance spectra. The experimental optical spectra taken from the fabricated sample are shown in Figure 3b and were recorded with a suitably modified Fourier transform infrared spectrometer (FTIR)[55] that was coupled to a microscope. Again, the lighter-colored curves correspond to spectra taken with the sandwich layer in the amorphous state. Because as-deposited GST-326 is amorphous, these were taken right after fabrication. Here, for proof-of-concept purposes we chose to thermally induce a transition to the crystalline state, which occurs for temperatures above the glass transition temperature of about 160 °C.[56] To that end, the entire sample was heated for 30 min at 180 °C under nitrogen atmosphere. The resulting transmittance and circular dichroism spectra of the crystalline state sample are presented as darker plots in Figure 3b. While the absolute transmittance values differ due to the fabricated sample consisting of disordered supercells leading to lower surface coverage than in the simulated periodic case, it is remarkable that the predicted giant shift of 18% is also experimentally realized. Previous studies[19] pointed out that simulations are typically merely interpreted as upper bounds to the shift. The excellent match of the magnitude of the shift can be possibly attributed to the fact that the GST-326 layer is completely surrounded by protective layers thus preventing degradation, for example, through oxidation and diffusion of gold during the switching process. Conventionally, such layers are avoided in order to ensure direct contact of the phase change material with the plasmonic nanostructures that are to be actuated.[57] The reasoning is that this maximizes the interaction of the near-fields in the vicinity of the antenna with the change in the refractive index environment. However, we are able to obtain shifting values that are comparable to literature values of systems that employed direct contact geometry. The reason for this is to be found in the coupled nanorod, that is, dimer configuration that results in higher field enhancements at the gap than at the ends of individual nanoantennas. Nevertheless, both simulated and experimental cases can be seen as boundaries to the tuning range of the transmittance and CD spectra in the sense that all intermediate states can be continuously achieved through adjusting the amount of heat deposited in the phase change layer.[58,59] This is because crystallization in the material takes place as a nucleation process[60] where evenly distributed small crystallites form that subsequently grow larger and finally merge to one homogeneous film.[61] Any of these nucleation stages is stable in itself and the plasmonic structure responds to an average dielectric constant of its surrounding that could be determined for instance by using Maxwell–Garnett theory.[62] This effect has been experimentally demonstrated for achiral planar plasmonic systems.[63]

Next, we want to emphasize the application potential beyond spectral tunability and demonstrate that indeed the wavelength tunability can be utilized to obtain a reversal in the sign of the circular dichroism signal. In the spectral region around 4150 nm where the CD peak is initially located, only very little CD response remains once the phase change material has been actuated, which is only possible due to the giant shift that the chiral dimer system undergoes. A smaller shift would not be able to push the entire CD signal out of the initial spectral

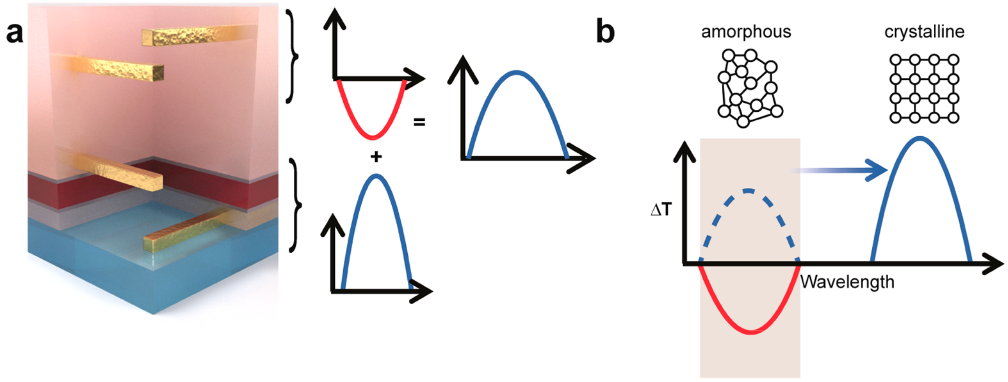

Figure 4. Switchable chirality concept. (a) A right-handed active chiral dimer is cascaded with a left-handed passive chiral dimer of half its CD amplitude. The overall CD response is half that of the right handed chiral dimer. (b) Thermal switching of the active chiral dimer shifts its CD signal red and exposes the underlying left-handed bias CD signal. The CD signal at the original wavelength region switches its sign.

range since plasmon resonance peaks and therefore their associated CD spectra are tied together, exhibiting relatively large full width at half-maximum values. We can utilize this unique situation to construct a scheme that is laid out in Figure 4a, which employs a bias layer to convert the spectral shift to a switching of the CD signal. Given a right-handed active chiral dimer (lower nanorod pair with sandwich layer) with a positive CD signal, we can design a left-handed passive chiral dimer (upper nanorod pair without sandwich layer) that possesses a negative CD signal of half the amplitude. As long as these two systems are separated by a distance that is sufficiently large (>200 nm) to avoid near-field coupling, the resulting CD spectra of light passing through both systems will be the sum of the individual CD spectra.[64] In the present case, the compound system possesses a positive CD signal of half the amplitude of the active chiral dimer. When this device is subjected to thermal actuation, the positive CD signal of the right-handed active dimer will shift away to the red, thus completely exposing the underlying negative CD signal. Overall this then appears like a switch in the CD signal at the original spectral position. The compound system can be viewed as an optical device that can switch its CD response. Because it does not matter for applications through which underlying physical mechanism right- or left-circularly polarized light is preferentially transmitted, the effect of a configurational change from a right-handed to a left-handed plasmonic enantiomer can thus be created through precise design of a bias layer that is overlaid with an active chiral metamaterial of high tuning range.

To experimentally demonstrate this concept, we carried out a parameter sweep of various passive chiral dimers in our numerical full-field simulation technique to find a suitable parameter set that has roughly half the CD signal of the active chiral dimer. We first varied the nanorod length to spectrally match the position of the active chiral metamaterial layer in the amorphous case (4.15 μm) and subsequently varied the interlayer separation between the nanorods to tailor the strength of the CD signal.[33] The best match was obtained for nanorods with length l = 800 nm, width w = 40 and thickness t = 40 nm that were vertically separated by d = 60 nm. The results are shown on the left in Figure 5a. Subsequently, a corresponding sample with the same parameters was fabricated and the CD spectrum was recorded. Note that here we used a periodic arrangement of the supercell with p = 1800 nm in both simulation and experiment because the comparably low refractive index of PC403 already prevents the formation of Rayleigh anomalies in the MIR for the chosen periodicity. The remarkable agreement in shape and amplitude of the resulting experimental data with the simulated data stems from the fact that the fabrication process for the passive chiral dimer is highly optimized and very well controlled. Figure 5b shows the overall optical response of the bias layer overlaid with the active chiral dimer. As designed, the CD signal at 4200 nm in the amorphous state is exactly opposite to the CD signal in the crystalline state for both fabricated enantiomers.

In summary, we have demonstrated for the first time a tunable chiral metamaterial that operates in the mid-IR spectral region with a tuning range from 4.15 to 4.90 μm. Subsequently, we have shown how to use this feature together with a bias layer to achieve a sign flip in the CD signal. Both functionalities have been achieved through easy-to-fabricate layered geometries without free-standing or moving parts. Here, for proof-of-concept purposes we only thermally induced a one-directional phase change from the amorphous to the crystalline state. However, it is well-known that GST can be electrically and optically switched on ultrafast time scales.[65,66] Our design that includes a continuous layer of GST can be modified to only incorporate patches of GST at the ends of the nanorods, which would ensure small enough volumes for electrical switching while retaining the wavelength tuning effect for the plasmon resonance. For optical switching no further modification of the geometry is needed, as large-area fs-switching of GST has been demonstrated already.[67] Therefore, our work opens up a path for high-frequency polarization modulation in the mid-infrared spectral region that would be highly beneficial for applications such as thermal imaging, polarization sensitive detection, and stereo display technologies. Most importantly, the phase change material GST-326 need not be restricted to active plasmonics applications where only the resonance wavelength is tuned via the change in the nanostructure dielectric environment. Moreover, it can be broadly employed as part of functionally complex but structurally simple designs that offer polarization engineering capabilities in the mid-infrared spectral region.

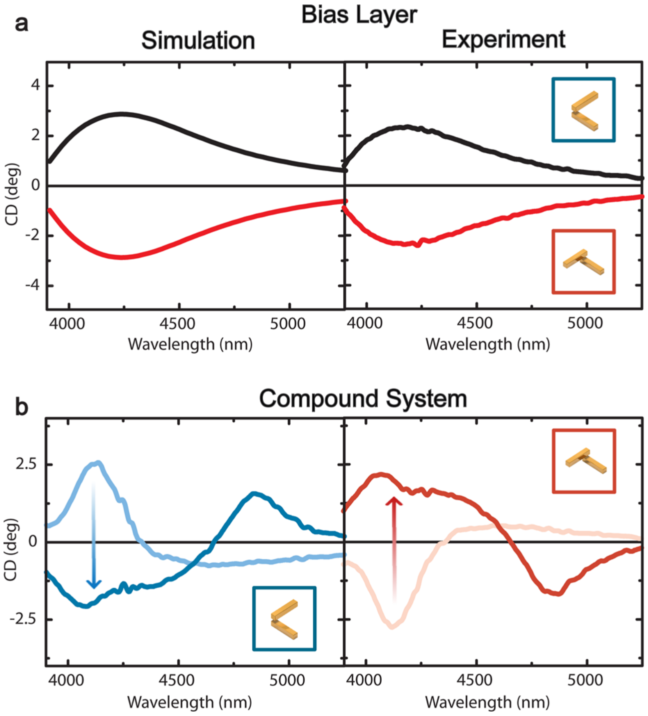

Figure 5. Switchable chirality. (a) Simulated and measured differential transmittance spectra $T_{\mathrm{RCP}}-T_{\mathrm{LCP}}$ of circularly polarized light for both enantiomers. (b) Experimental results for the cascaded system consisting of the active chiral dimer and the opposite-handed passive bias dimer. The CD signal switches its sign symmetrically for both opposite-handedness combinations of the active chiral dimer with the passive chiral bias layer.

AUTHOR INFORMATION

Corresponding Author

*E-mail: x.yin@pi4.uni-stuttgart.de.

Author Contributions

X.Y. and H.G. conceived the idea and planned the experiments. X.Y. carried out the fabrication and experiment. X.Y., M.S., and A.T. simulated the structures. A.-K.M., M.W., and T.T. carried out and supervised the GST deposition. X.Y. and H.G. wrote the manuscript. All authors contributed to revise the manuscript.

Notes

The authors declare no competing financial interest.

■ ACKNOWLEDGMENTS

The authors gratefully acknowledge financial support by the ERC Advanced Grant (COMPLEXPLAS), BMBF (13N9048 and 13N10146), the Baden Württemberg Stiftung (Internationale Spitzenforschung II), DFG (SPP1391, FOR730, and GI 269/11-1) and SFB 917 (Nanoswitches). X.Y. additionally acknowledges financial support by the Carl-Zeiss-Stiftung and would like to thank the Max-Planck-Institute for Solid State Research, in particular Jürgen Weis and Thomas Reindl, for cleanroom access and helpful discussions.

■ REFERENCES

(1) Zheludev, N. I.; Kivshar, Y. S. *Nat. Mater.* **2012**, *11*, 917−924.
(2) Pryce, I. M.; Aydin, K.; Kelaita, Y. A.; Briggs, R. M.; Atwater, H. A. *Nano Lett.* **2010**, *10*, 4222−4227.
(3) Ou, J. Y.; Plum, E.; Jiang, L.; Zheludev, N. I. *Nano Lett.* **2011**, *11*, 2142−2144.
(4) Papasimakis, N.; Luo, Z.; Shen, Z. X.; De Angelis, F.; Di Fabrizio, E.; Nikolaenko, A. E.; Zheludev, N. I. *Opt Express* **2010**, *18*, 8353−8359.
(5) Yao, Y.; Kats, M. A.; Genevet, P.; Yu, N.; Song, Y.; Kong, J.; Capasso, F. *Nano Lett.* **2013**, *13*, 1257−1264.
(6) Yao, Y.; Kats, M. A.; Shankar, R.; Song, Y.; Kong, J.; Loncar, M.; Capasso, F. *Nano Lett.* **2014**, *14*, 214−219.
(7) Fang, Z.; Wang, Y.; Schlather, A. E.; Liu, Z.; Ajayan, P. M.; de Abajo, F. J. G.; Nordlander, P.; Zhu, X.; Halas, N. J. *Nano Lett.* **2014**, *14*, 299−304.
(8) Chen, H.-T.; Padilla, W. J.; Zide, J. M. O.; Gossard, A. C.; Taylor, A. J.; Averitt, R. D. *Nature* **2006**, *444*, 597−600.
(9) Padilla, W. J.; Taylor, A. J.; Highstrete, C.; Lee, M.; Averitt, R. D. *Phys. Rev. Lett.* **2006**, *96*, 107401.
(10) Chen, H.-T.; O'Hara, J. F.; Azad, A. K.; Taylor, A. J.; Averitt, R. D.; Shrekenhamer, D. B.; Padilla, W. J. *Nat. Photonics* **2008**, *2*, 295−298.
(11) Tao, H.; Strikwerda, A. C.; Fan, K.; Padilla, W. J.; Zhang, X.; Averitt, R. D. *Phys. Rev. Lett.* **2009**, *103*, 147401.
(12) Luther, J. M.; Jain, P. K.; Ewers, T.; Alivisatos, A. P. *Nat. Mater.* **2011**, *10*, 361−366.
(13) Dicken, M. J.; Aydin, K.; Pryce, I. M.; Sweatlock, L. A.; Boyd, E. M.; Walavalkar, S.; Ma, J.; Atwater, H. A. *Opt. Express* **2009**, *17*, 18330−18339.
(14) Kats, M. A.; Sharma, D.; Lin, J.; Genevet, P.; Blanchard, R.; Yang, Z.; Qazilbash, M. M.; Basov, D. N.; Ramanathan, S.; Capasso, F. *Appl. Phys. Lett.* **2012**, *101*, 221101.
(15) Kats, M. A.; Blanchard, R.; Genevet, P.; Yang, Z.; Qazilbash, M. M.; Basov, D. N.; Ramanathan, S.; Capasso, F. *Opt. Lett.* **2013**, *38*, 368−370.
(16) Soares, B.; Jonsson, F.; Zheludev, N. *Phys. Rev. Lett.* **2007**, *98*, 153905.
(17) Vivekchand, S. R. C.; Engel, C. J.; Lubin, S. M.; Blaber, M. G.; Zhou, W.; Suh, J. Y.; Schatz, G. C.; Odom, T. W. *Nano Lett.* **2012**, *12*, 4324−4328.
(18) Strohfeldt, N.; Tittl, A.; Schäferling, M.; Neubrech, F.; Kreibig, U.; Griessen, R.; Giessen, H. *Nano Lett.* **2014**, *14*, 1140−1147.
(19) Gholipour, B.; Zhang, J.; MacDonald, K. F.; Hewak, D. W.; Zheludev, N. I. *Adv. Mater.* **2013**, *25*, 3050−3054.
(20) Michel, A.-K. U.; Chigrin, D. N.; Maß, T. W. W.; Schönauer, K.; Salinga, M.; Wuttig, M.; Taubner, T. *Nano Lett.* **2013**, *13*, 3470−3475.
(21) Cao, T.; Wei, C.-W.; Simpson, R. E.; Zhang, L.; Cryan, M. J. *Sci. Rep.* **2014**, *4*, 3955.
(22) Papakostas, A.; Potts, A.; Bagnall, D.; Prosvirnin, S.; Coles, H.; Zheludev, N. *Phys. Rev. Lett.* **2003**, *90*, 107404.
(23) Kuwata-Gonokami, M.; Saito, N.; Ino, Y.; Kauranen, M.; Jefimovs, K.; Vallius, T.; Turunen, J.; Svirko, Y. *Phys. Rev. Lett.* **2005**, *95*, 227401.
(24) Plum, E.; Fedotov, V. A.; Schwanecke, A. S.; Zheludev, N. I.; Chen, Y. *Appl. Phys. Lett.* **2007**, *90*, 223113.
(25) Hentschel, M.; Schäferling, M.; Weiss, T.; Liu, N.; Giessen, H. *Nano Lett.* **2012**, *12*, 2542−2547.
(26) Kuzyk, A.; Schreiber, R.; Fan, Z.; Pardatscher, G.; Roller, E.-M.; Högele, A.; Simmel, F. C.; Govorov, A. O.; Liedl, T. *Nature* **2012**, *483*, 311−314.
(27) Guerrero-Martínez, A.; Auguié, B.; Alonso-Gómez, J. L.; Džolić, Z.; Gómez-Graña, S.; Žinić, M.; Cid, M. M.; Liz-Marzán, L. M. *Angew. Chem., Int. Ed.* **2011**, *50*, 5499−5503.
(28) Decker, M.; Klein, M. W.; Wegener, M.; Linden, S. *Opt. Lett.* **2007**, *32*, 856−858.
(29) Decker, M.; Ruther, M.; Kriegler, C. E.; Zhou, J.; Soukoulis, C. M.; Linden, S.; Wegener, M. *Opt. Lett.* **2009**, *34*, 2501−2503.
(30) Gansel, J. K.; Thiel, M.; Rill, M. S.; Decker, M.; Bade, K.; Saile, V.; Von Freymann, G.; Linden, S.; Wegener, M. *Science* **2009**, *325*, 1513−1515.
(31) Helgert, C.; Pshenay-Severin, E.; Falkner, M.; Menzel, C.; Rockstuhl, C.; Kley, E.-B.; Tünnermann, A.; Lederer, F.; Pertsch, T. *Nano Lett.* **2011**, *11*, 4400−4404.
(32) Frank, B.; Yin, X.; Schäferling, M.; Zhao, J.; Hein, S. M.; Braun, P. V.; Giessen, H. *ACS Nano* **2013**, *7*, 6321−6329.
(33) Yin, X.; Schäferling, M.; Metzger, B.; Giessen, H. *Nano Lett.* **2013**, *13*, 6238−6243.
(34) Kanda, N.; Konishi, K.; Kuwata-Gonokami, M. *Opt. Lett.* **2009**, *34*, 3000−3002.
(35) Zhang, S.; Park, Y.-S.; Li, J.; Lu, X.; Zhang, W.; Zhang, X. *Phys. Rev. Lett.* **2009**, *102*, 023901.
(36) Zhao, R.; Koschny, T.; Soukoulis, C. M. *Opt Express* **2010**, *18*, 14553−14567.
(37) Aschaffenburg, D. J.; Williams, M. R. C.; Talbayev, D.; Santavicca, D. F.; Prober, D. E.; Schmuttenmaer, C. A. *Appl. Phys. Lett.* **2012**, *100*, 241114.
(38) Rogacheva, A. V.; Fedotov, V. A.; Schwanecke, A. S.; Zheludev, N. I. *Phys. Rev. Lett.* **2006**, *97*, 177401.
(39) Kuzyk, A.; Schreiber, R.; Zhang, H.; Govorov, A. O.; Liedl, T.; Liu, N. *Nat. Mater.* **2014**, *13*, 862−866.
(40) Zhang, S.; Zhou, J.; Park, Y.-S.; Rho, J.; Singh, R.; Nam, S.; Azad, A. K.; Chen, H.-T.; Yin, X.; Taylor, A. J.; Zhang, X. *Nat. Commun.* **2012**, *3*, 942.
(41) Kenanakis, G.; Zhao, R.; Katsarakis, N.; Kafesaki, M.; Soukoulis, C. M.; Economou, E. N. *Optically controllable THz chiral metamaterials*; Optical Society of America: Washington, DC, 2014; Vol. 22, pp 12149−12159.
(42) Lv, T. T.; Zhu, Z.; Shi, J. H.; Guan, C. Y.; Wang, Z. P.; Cui, T. J. *Opt. Lett.* **2014**, *39*, 3066−3069.
(43) Kanda, N.; Konishi, K.; Kuwata-Gonokami, M. *Opt. Lett.* **2014**, *39*, 3274−3277.
(44) Stanley, R. *Nat. Photonics* **2012**, *6*, 409−411.
(45) Hosseini, P.; Wright, C. D.; Bhaskaran, H. *Nature* **2014**, *511*, 206−211.
(46) Homola, J.; Piliarik, M. In *Surface Plasmon Resonance Based Sensors*; Springer Series on Chemical Sensors and Biosensors; Springer: Berlin, 2006; Vol. 4, pp 45−67.
(47) Anker, J. N.; Hall, W. P.; Lyandres, O.; Shah, N. C.; Zhao, J.; Van Duyne, R. P. *Nat. Mater.* **2008**, *7*, 442−453.
(48) Cao, T.; Zhang, L.; Simpson, R. E.; Wei, C.; Cryan, M. J. *Opt Express* **2013**, *21*, 27841−27851.
(49) Auguié, B.; Lorenzo Alonso-Gomez, J.; Guerrero-Martínez, A.; Liz-Marzán, L. M. *J. Phys. Chem. Lett.* **2011**, *2*, 846−851.
(50) Svirko, Y.; Zheludev, N.; Osipov, M. *Appl. Phys. Lett.* **2001**, *78*, 498−498.
(51) Liu, N.; Guo, H.; Fu, L.; Kaiser, S.; Schweizer, H.; Giessen, H. *Nature* **2007**, *7*, 31−37.
(52) Nau, D.; Schönhardt, A.; Bauer, C.; Christ, A.; Zentgraf, T.; Kuhl, J.; Klein, M.; Giessen, H. *Phys. Rev. Lett.* **2007**, *98*, 133902.

(53) Tittl, A.; Harats, M. G.; Walter, R.; Yin, X.; Schäferling, M.; Liu, N.; Rapaport, R.; Giessen, H. *ACS Nano* **2014**, *8*, 10885−10892.
(54) Weiss, T.; Granet, G.; Gippius, N. A.; Tikhodeev, S. G.; Giessen, H. *Opt Express* **2009**, *17*, 8051−8061.
(55) Korte, E. H. *Appl. Spectrosc.* **1978**, *32*, 568−572.
(56) Shportko, K.; Kremers, S.; Woda, M.; Lencer, D.; Robertson, J.; Wuttig, M. *Nat. Mater.* **2008**, *7*, 653−658.
(57) Cao, T.; Wei, C.; Simpson, R. E.; Zhang, L.; Cryan, M. J. *Sci. Rep.* **2013**, *4*, 4463−4463.
(58) Wang, R.; Wei, J.; Fan, Y. *Opt Express* **2014**, *22*, 4973−4984.
(59) Wang, Q.; Maddock, J.; Rogers, E. T. F.; Roy, T.; Craig, C.; MacDonald, K. F.; Hewak, D. W.; Zheludev, N. I. *Appl. Phys. Lett.* **2014**, *104*, 121105.
(60) Hegedüs, J.; Elliott, S. R. *Nat. Mater.* **2008**, *7*, 399−405.
(61) Raoux, S.; Wuttig, M. *Phase Change Materials*; Raoux, S., Wuttig, M., Eds.; Springer Science & Business Media: Boston, MA, 2010.
(62) Maier, S. A. *Plasmonics: Fundamentals and Applications*, 1st ed.; Springer: New York, 2007.
(63) Chen, Y. G.; Kao, T. S.; Ng, B.; Li, X.; Luo, X. G.; Luk'yanchuk, B.; Maier, S. A.; Hong, M. H. *Opt Express* **2013**, *21*, 13691−13698.
(64) Hentschel, M.; Schäferling, M.; Metzger, B.; Giessen, H. *Nano Lett.* **2013**, *13*, 600−606.
(65) Bruns, G.; Merkelbach, P.; Schlockermann, C.; Salinga, M.; Wuttig, M.; Happ, T. D.; Philipp, J. B.; Kund, M. *Appl. Phys. Lett.* **2009**, *95*, 043108.
(66) Loke, D.; Lee, T. H.; Wang, W. J.; Shi, L. P.; Zhao, R.; Yeo, Y. C.; Chong, T. C.; Elliott, S. R. *Science* **2012**, *336*, 1566−1569.
(67) Michel, A.-K. U.; Zalden, P.; Chigrin, D. N.; Wuttig, M.; Lindenberg, A. M.; Taubner, T. *ACS Photonics* **2014**, *1*, 833−839.